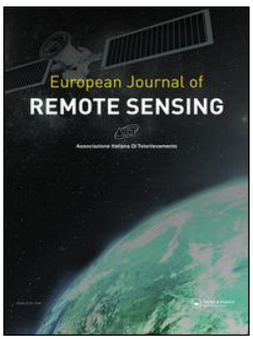

European Journal of Remote Sensing

ISSN: (Print) (Online) Journal homepage: https://www.tandfonline.com/loi/tejr20

Prediction of forest canopy fuel parameters in managed boreal forests using multispectral and unispectral airborne laser scanning data and aerial images

Matti Maltamo , J. Räty , L. Korhonen , E. Kotivuori , M. Kukkonen , H. Peltola , J. Kangas & P. Packalen

To cite this article: Matti Maltamo , J. Räty , L. Korhonen , E. Kotivuori , M. Kukkonen , H. Peltola , J. Kangas & P. Packalen (2020) Prediction of forest canopy fuel parameters in managed boreal forests using multispectral and unispectral airborne laser scanning data and aerial images, European Journal of Remote Sensing, 53:1, 245-257, DOI: 10.1080/22797254.2020.1816142

To link to this article: https://doi.org/10.1080/22797254.2020.1816142

Published online: 08 Sep 2020.

EUROPEAN JOURNAL OF REMOTE SENSING
2020, VOL. 53, NO. 1, 245–257
https://doi.org/10.1080/22797254.2020.1816142

Taylor & Francis
Taylor & Francis Group

Prediction of forest canopy fuel parameters in managed boreal forests using multispectral and unispectral airborne laser scanning data and aerial images

Matti Maltamo[a], J. Räty[b], L. Korhonen[a], E. Kotivuori[a], M. Kukkonen[a], H. Peltola[a], J. Kangas[a] and P. Packalen[a]

[a]School of Forest Sciences, University of Eastern Finland, Joensuu, Finland; [b]Division of Forest and Forest Resources, National Forest Inventory, Norwegian Institute of Bioeconomy Research (NIBIO), Ås, Norway

ABSTRACT

This study evaluated the suitability of different airborne laser scanning (ALS) datasets for the prediction of forest canopy fuel parameters in managed boreal forests in Finland. The ALS data alternatives were leaf-off and leaf-on unispectral and leaf-on multispectral data, alone and combined with aerial images. Canopy fuel weight, canopy base height, biomass of living and dead trees, and height and biomass of the understory tree layer were predicted using regression analysis. The considered categorical forest parameters were dominant tree species, site fertility and vertical forest structure layers. The canopy fuel weight was modeled based on crown biomass with an RMSE% value of 20–30%. The canopy base heights were predicted separately for pine and spruce stands with satisfactory results the RMSE% values being 9–10% and 15–17%, respectively. Following the initial classification of the existence of an understory layer (with kappa-values of 0.47–0.53), the prediction of understory height performed well (RMSE% 20–25%) but the understory biomass was predicted with larger RMSE% values (about 60–70%). Site fertility was classified with kappa-values of 0.5–0.6. The most accurate results were obtained using multispectral ALS data, although the differences between the datasets were minor.

ARTICLE HISTORY
Received 11 July 2020
Revised 20 August 2020
Accepted 25 August 2020

KEYWORDS
Forest fire; forest structure; boreal forests; fuel models; forest fuel parameters; LiDAR

Introduction

Forest fires are one of the greatest natural hazards faced by boreal forests. However, fire is also a natural phenomenon and is an important factor in maintaining biodiversity and in natural regeneration (Esseen et al., 1997; Koutsias & Karteris, 2003). In Nordic countries, such as Finland, approximately 1000 forest fires occur, on average, each year (Lehtonen et al., 2016). During 2015, the annual damaged forest area by forest fires in Central-East and South-West Europe was 374,200 and 234,400 hectares, respectively, whereas the corresponding area in North-Europe was only 2 000 hectares (Forest Europe, 2015). The area burnt in Finland is relatively small because of active fire suppression, and the heterogeneity of forested areas with numerous lakes and swamps, and a dense forest road network, which create natural obstacles to fire spread (Lehtonen et al., 2014). In contrast, large wildfires are common along the southern edge of boreal forests in Russia, for example. Nonetheless, in August 2014, a large forest fire of approximately 150,000 hectares occurred and rapidly spread in Västmanland, Sweden (Bohlin et al., 2017). Similarly, during a hot dry period in the summer of 2018, several substantial forest fires occurred in Sweden and in Finland, providing further evidence of the increasing susceptibility of managed boreal forests to fire. The risk of forest fires is also expected to increase in Finland and elsewhere in the boreal zone under a warming climate, due to increased frequency of drought periods (Lehtonen et al., 2014, 2016; Ruosteenoja et al., 2018).

The factors that affect forest fire risk include weather, topography and fuels, i.e. materials that can burn during a fire (Holsinger et al., 2016; Moritz et al., 2011). Remote sensing has been widely used to characterize forest fire risks, as it is an ideal tool for predicting fuel availability, monitoring fires, mapping burnt areas and for the monitoring of regeneration after fire (Jones & Vaughan, 2012). In particular, optical satellite images usually cover large areas, provide spatial representation of vegetation, and are available multi-temporally. However, a disadvantage of optical satellite images is that they are not usually able to characterize the vertical forest structure, i.e. properties related to height (e.g. Arroyo et al., 2008; Chirici et al., 2013). These limitations can be overcome by using 3D airborne laser scanning (ALS) data in a forest fuel context (Andersen et al., 2005; Chirici et al., 2013; see also text book chapter by Gajardo et al., 2014), either at an individual tree-level or at the area (plot/cell/stand) level, depending on the properties of the data and information needs of the application. In addition, ALS data provide accurate and detailed information on topography. Therefore, ALS information can be effectively used to map fuel types and to

CONTACT Matti Maltamo matti.maltamo@uef.fi School of Forest Sciences, University of Eastern Finland, Joensuu 80101, Finland

estimate canopy fuel parameters (Andersen et al., 2005; Arroyo et al., 2008; Mutlu et al., 2008; Riaño et al., 2003).

Fuel type mapping is critical for spatial modeling of forest fire behavior (Chirici et al., 2013). Forest fire behavior is predicted in different forest fire simulators where canopy fuel parameters are used as input variables (e.g. Andersen et al., 2005). In general, fuel type mapping can be understood as the classification of an area of interest according to vegetation species, form, size, arrangement and continuity of fuels (Gajardo et al., 2014; see also Merrill & Alexander, 1987). Trees, understory, shrub, grass, brush and litter are considered as different fuel types (Jones & Vaughan, 2012). Fuel type mapping is also a type of forest area stratification as segmentation to different-sized objects, such as trees, tree groups or stands, in a forest inventory. ALS data stratifies the area of interest by considering the horizontal and vertical structures of the forest as pre-processing steps, before fuel type mapping with ALS features is then conducted (Mutlu et al., 2008; Seielstad & Queen, 2003).

The most often considered canopy fuel parameter is canopy bulk density (CBD), which can be defined as the mass of available canopy fuel (canopy fuel weight) per defined chosen unit canopy volume (Gajardo et al., 2014). This attribute is an input variable in many fire behavior models. When the canopy fuel weight is calculated, only foliage biomass, or both foliage and branches, are considered. There are different ways to utilize ALS data to predict CBD. For example, Riaño et al. (2003) predicted foliage biomass by means of ALS data and calculated canopy volume from an ALS point cloud. They derived CBD by dividing the biomass estimate by the canopy volume estimate. Similarly, Andersen et al. (2005) separately predicted canopy fuel weight (biomass) and CBD. Moreover, ALS height distribution can be assigned to height bins to achieve a 3D presentation of CBD. Numerous studies have employed ALS to predict foliage biomass for purposes other than fuel parameters, such as bioenergy, (e.g. Hauglin et al., 2012; Kotamaa et al., 2010; Lim & Treitz, 2004). Usually the accuracy of these predictions has been found suitable for the operational use.

Another important canopy fuel parameter is canopy base height (CBH). In a forest fire context, this attribute is the lowest point in the canopy where there is sufficient canopy fuel to cause vertical fire spread. However, there are many different definitions for CBH, e.g. the vertical distance from the ground to the live crown base (Finney, 1998), or some minimum limit in vertical CBD distribution (Andersen et al., 2005). CBH can be estimated rather accurately according to the vertical point cloud properties of ALS data (e.g. Maltamo et al., 2010, 2018; Morsdorf et al., 2004; Riaño et al., 2003; Vauhkonen, 2010) or by regression analysis (Næsset & Økland, 2002; Andersen et al., 2005; Maltamo et al., 2018). As with canopy foliage, many different applications exist for ALS-based CBH estimates, such as forest biomass prediction, growth and yield models, and timber quality (Repola, 2009; Salminen et al., 2005; Wall et al., 2004).

The third most important forest fuel parameter is the surface canopy height (SCH) (e.g. Andersen et al., 2005; Gajardo et al., 2014; Mutlu et al., 2008). This parameter can be defined as the height of the fuel layer below the canopy but above ground level. Usually this layer consists of shrubs and understory trees beneath the dominant layer. In some cases, the layer can be directly discriminated from ALS data (Estornell et al., 2011; Riaño et al., 2007), although this usually leads to underestimation of the surface height. It is also possible to initially detect the existence of the understory layer from the properties of the vertical distribution of ALS echoes (Hill & Broughton, 2009; Sumnall et al., 2016), and to then predict the attributes of interest (Maltamo et al., 2005). The variation in vertical forest structure described by ALS has also been widely examined from a biodiversity point of a view (Miura & Jones, 2010; Valbuena et al., 2016).

In many studies, discrete return ALS data have been combined with spectral data to improve the prediction accuracy of forest fuel parameters (Erdody & Moskal, 2010; Mutlu et al., 2008). However, the improvement associated with the prediction errors is usually minor. In addition, full waveform ALS data have been applied (Peterson et al., 2007). Recently, commercial airborne multispectral ALS systems, which are capable of providing a reflective metric (echo intensity) over several wavelengths, have been introduced and tested to discriminate between tree species at the tree- or plot-level (Axelsson et al., 2018; Budei et al., 2018; Kukkonen et al., 2019a; Yu et al., 2017).

The aim of this study was to evaluate the suitability of different ALS datasets and aerial images for the prediction of forest canopy fuel-related parameters at the plot-level in managed middle-aged and mature boreal forests. Canopy fuel weight, CBH, biomass of living and dead trees, and height and biomass of the understory tree layer were predicted using regression analysis. The considered categorical forest parameters were dominant tree species, site fertility and vertical forest structure layers. All predictions and classifications were cross-validated using relative root-mean-square error (RMSE%) and kappa-values.

Material and methods

Study area

The study area (43,200 hectares) is located in eastern Finland (Figure 1). It extends over the regions of North Karelia and Southern Savonia and includes the

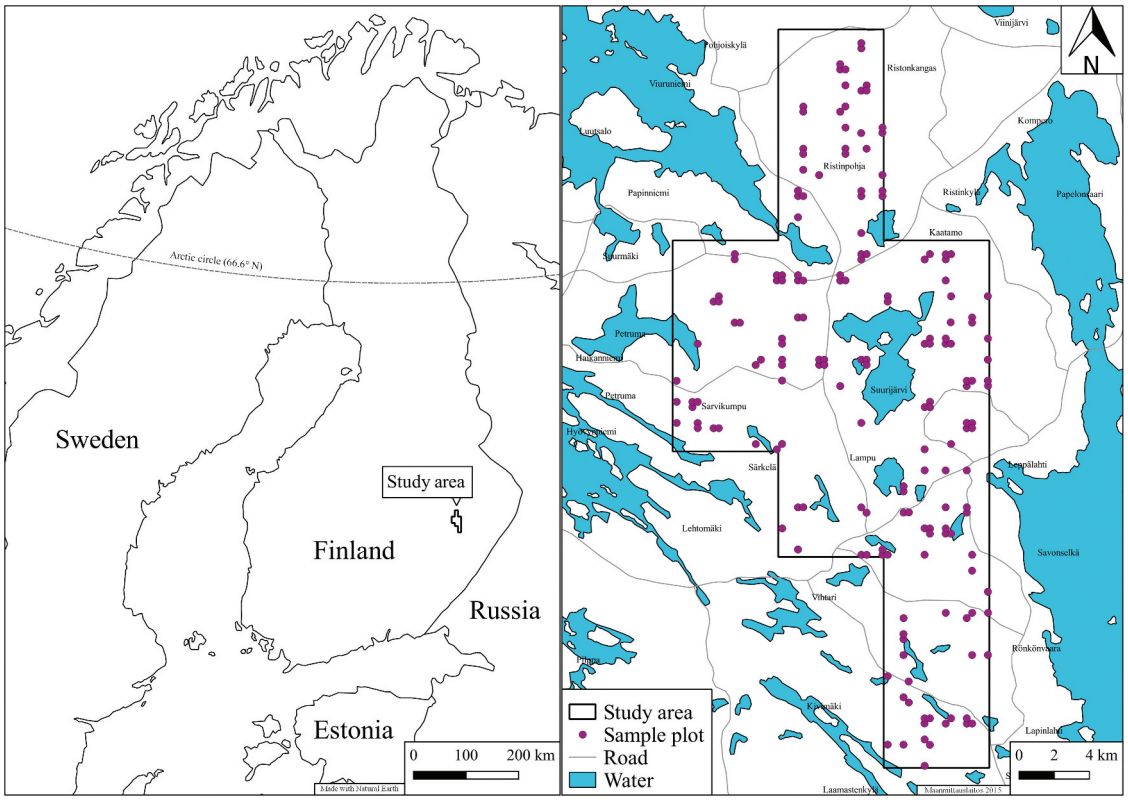

Figure 1. Location of the study area and sample plots in eastern Finland.

municipalities of Heinävesi, Liperi, Outokumpu and Savonlinna. The study area includes managed boreal forests dominated by coniferous tree species (Räty et al., 2019). The main tree species in the area are Norway spruce (*Picea abies* [L.] Karst.), Scots pine (*Pinus sylvestris* [L.]), silver birch (*Betula pendula* Roth) and downy birch (*B. pubescens* Ehrh.). Other deciduous tree species, such as grey alder (*Alnus incana* [L.] Moench) and aspen (*Populus tremula* [L.]) grow in the lower canopy layers. The majority of the plots were located in middle-aged forests (74%) and the remainder in mature forests.

Field data

We used 179 fixed radius sample plots of 9 m in this study (see Figure 1). The plot measurements were conducted between June and September 2016. Plot locations were selected using systematic cluster sampling with random start. The distance between clusters was 1200 m. The cluster was quare-shaped with a side length of 300 m. Sample plots were placed in the corners of clusters. Finally, a subset of clusters was selected to the sample and measured. Plots located in seedling and sapling stands were excluded. Plot locations were positioned by means of a global navigation satellite system (GNSS). The GNSS data were corrected afterwards using reference stations. Diameter at breast height (DBH), crown base height and tree height were measured from all trees having DBH ≥ 5 cm. Trees species were also determined from measured trees. Most important plot attributes are shown in Table 1. Categorical variables site fertility class and existence of understory layer were determined at the plot-level. Site fertility was classified as grove (*Oxalis-Maianthemum* type, OMaT), fertile (*Oxalis-Myrtillus* type, OMT), moderate (*Vaccinium-Myrtillus* type, MT) or poor (*Vaccinium vitis idaea* type, VT) types, according to the classification by Cajander (1926). In the case of an existing understory layer, dominant species, height and number of stems were recorded at the plot-level.

Table 1. Mean, minimum, maximum and standard deviation (sd) of the main forest attributes. AGB denotes aboveground biomass.

Attribute	Mean	Sd	Min	Max
AGB, living trees, Mg·ha^{-1}	110.7	47.9	27.4	410.0
AGB, dead trees, Mg·ha^{-1}	1.0	2.7	0.0	22.5
Needle biomass, Mg·ha^{-1}	7.2	3.8	1.9	19.3
Crown biomass, Mg·ha^{-1}	24.7	11.4	7.1	66.9
Canopy base height (pine), m	9.9	2.6	4.4	18.9
Canopy base height (spruce), m	6.5	2.1	1.4	10.6
Height of understory, dm	21.2	6.6	7.0	40.0
AGB of understory, Mg·ha^{-1}	1.3	1.0	0.2	5.3

Field data preprocessing

Different biomass characteristics were calculated at the tree-level. Deciduous species were assigned to a single group, as a biomass model only exists for birch. Thus,

three tree species groups were established: pine, spruce, and deciduous. DBH and height measurements were used to calculate the total aboveground biomass (AGB) for living and dead trees (Repola, 2008, 2009). In addition to DBH and height, crown base height was used as a predictor variable when calculating crown (foliage and branches) biomass. Finally, the following attributes were computed at the plot-level per hectare: AGB for both living and dead trees, foliage (needles) biomass, crown biomass, basal area-weighted CBH and AGB of the understory layer. Biomass for the understory layer was approximated using species, height/DBH and stand density information using the models described by Repola (2008, 2009)).

Considered fuel parameters were as follows: (1) site fertility in two classes: rich, n = 28 (OMAT and OMT types) and dry, n = 151 (MT and VT types); (2) the existence of SCH in two classes: present, n = 54 or absent, n = 125; (3) the foliage (needles) and crown (foliage and branches) biomass as estimates of canopy fuel weight; and (4) CBH was considered separately in pine (n = 91) and spruce (n = 77) dominated stands since this attribute differed considerably between stands (see Table 1). Thus, additional classification was required to separate pine and spruce dominated stands. In our calculations, deciduous stands were combined with the pine dominated stand, since the CBH values of the deciduous stands were similar to the values observed in pine stands. Furthermore, (5) height and (6) AGB of existing SCH, (7) AGB of living (AGB_l) and (8) AGB of dead trees (AGB_d) were considered.

ALS datasets

Multispectral ALS data was collected at an altitude of 850 m above ground level with a Teledyne Optech Titan device (Geo3d.hr 2018). The data was collected in June 2016 under leaf-on conditions. The Teledyne Optech Titan measures up to four range and intensity measurements per pulse using the wavelengths 1550 nm, 1064 nm, and 532 nm for the first, second and third channel, respectively. The overlap of strips was 55% so most targets on the ground were scanned from two flight lines. In an average, the pulse density per flight line was 4.8 pulses per square meter for channels 1 and 2, and 3.7 for channel 3. We also used data from the second channel independently in our analysis. We call it as unispectral leaf-on ALS data onward.

Unispectral ALS data were collected under leaf-off conditions on 30 April–3 May 2016 with a Leica ALS60 device. The flying altitude was 2400 m above ground level and strip overlap was 20%. This configuration provided the pulse density of 0.8 pulses per square meter. The Leica ALS60 captures up to four echoes, including range and intensity measurements, for each emitted pulse. The ALS60 ALS system uses the 1064 nm wavelength.

The ALS echo heights were normalized to above ground level by subtracting the terrain level from the orthometric heights. This was done separately with multispectral (Optech Titan) and unispectral (Leica ALS60) ALS data. First ground echoes were filtered as explained in Axelsson (2000). Then ground echoes and Delaunay triangulation were used to interpolate a digital terrain model. This terrain model was subtracted from the initial orthometric heights. The lidar intensity values were range corrected as documented in Korpela et al. (2010). In corresponding forest area Kukkonen et al. (2019a) found that intensity correction had only very minor influence on the predictions.

Aerial imagery

Aerial images were acquired under leaf-on conditions on May 23–24, 2016. The aerial images were captured with a DMC Z/I Intergraph (01–0128) digital aerial camera. The images were taken from an altitude of 4100 m. This resulted in a ground sample distance of approximately 1.5 m. A lateral overlap was 30% and longitudinal overlap was 80%. The DMC Z/I has four multispectral bands (red, green, blue and nir) that have the resolution of 1920 × 3456 pixels. Bundle block adjustment with ground and tie points were used to determine external orientations in a standard manner. Images were not pansharpened or orthorectified, because DN values of aerial images were linked to ALS echoes and image features were computed from these, as explained in the section 2.4.

ALS and aerial image features

Three echo categories were formed from the original three echo categories: *first = first of many + only echoes*, and *last = last of many + only echoes*. In addition, intermediate echoes were used in the analysis, such as the one echo category. A set of features was computed for each field plot from the leaf-on multispectral ALS, leaf-on and leaf-off unispectral ALS, and aerial image datasets (Table 2). We used feature categories (I) channel-wise, (II) multicloud, (III) multiratio, and (IV) aerial image (Kukkonen et al., 2019a, 2019b). Channel-wise features included the height distribution and intensity features calculated separately from first (f), last (l) and intermediate (int) echoes by channel. Multicloud features included the above-mentioned features computed from the combined set of echoes from two or three channels. Multiratio features included the ratios of features calculated for the individual channels.

The features extracted from the aerial images were computed by the spectral bands: red, green, blue and

Table 2. Features extracted from airborne laser scanning (ALS) data and aerial images. Abbreviations: h = height; i = intensity; ai = aerial image; R = red; G = green; B = blue; N = near infra-red; DN = digital number. Abbreviations f, l and int (not shown in Table) denote variables computed from first, last and intermediate echo classes, respectively. Subscripts for the channels of the multispectral ALS data are 1550, 1064 and 532 for the first, second and third channel, respectively.

Feature	Description
I – Channel-wise	
hP10, hP20, …, hP90	Height percentiles
iP10, iP20, …, iP90	Intensity percentiles
hD1, hD2, hD5, hD10, hD15, hD20	Density at a fixed height
iMax, hMax	Maximum
iMin, hMin	Minimum
iStd, hStd	Standard deviation
iMed, hMed	Median
iMean, hMean	Mean
iSkew, hSkew	Skewness
iKurt, hKurt	Kurtosis
Prop	Echo class proportion
II – Multicloud	
I1550 + 1064; I1550 + 532; I1064 + 532; I1550 + 1064 + 532	Channel-wise Features (I) computed from combined set of echoes from different channels
III – Multiratio	
I1550/I1064; I1550/I532; I1064/I532,	Ratios of channel-wise features (I)
IV – Aerial image	
aiMax (B;G;R;N)	Maximum DN
aiMin (B;G;R;N)	Minimum DN
aiStd (B;G;R;N)	Standard deviation of DNs
aiMean (B;G;R;N)	Mean DN

near-infrared. The digital number (DN) values were fetched from the pixels of aerial images for each first ALS echo. The DN values were determined by projecting the first ALS echoes over the aerial images using the collinearity equations from photogrammetry. The mean DN value was first computed for each echo by iterating through all the overlapping images where an echo was visible. Aerial image features were calculated separately for each ALS dataset.

We established six feature groups that were separately used in the analyses. The groups were (1) unispectral leaf-on ALS (i.e. the second channel of multispectral ALS data), (2) the combination of unispectral leaf-on ALS and aerial images, (3) unispectral leaf-off ALS, (4) the combination of unispectral leaf-off ALS and aerial images, (5) multispectral leaf on ALS, and (6) multispectral leaf-on ALS and aerial images (Table 3).

Modelling and validation of fuel parameters

Linear discriminant analysis (LDA) was used to classify site fertility, the existence of SCH, and the main tree species. The LDA was carried out with equal prior probabilities of the class memberships using the LDA function in the MASS package (Venables & Ripley, 2002) in the R environment (R Core Team, 2019). Predictor variables of the classification models were selected using a simulated annealing (Kirkpatrick et al., 1983) optimization algorithm. The optimization commenced with a random set of predictor variable candidates. The set of predictor variables was modified during the optimization process by replacing some of the predictor variables in the current set. The number of predictor variables to be replaced with new variables decreased during the optimization. The aim of the optimization was to minimize the loss function that was an inversed kappa-value. The number of predictor variables in the models was five.

Table 3. Feature groups used in the variable selection. For the feature codes, please refer to Table 2.

Feature group	Features
Unispectral leaf-on ALS	I
Unispectral leaf-on ALS and aerial images	I and IV
Unispectral leaf-off ALS	I
Unispectral leaf-off ALS and aerial images	I and IV
Multispectral leaf-on ALS	I, II and III
Multispectral leaf-on ALS and aerial images	I, II, III and IV

In the parametric modelling approach, the relationship between remote sensing features and fuel parameters (CBH, needle and crown biomass, AGB_l and AGB_d, height and AGB of SCH) was characterized by means of linear regression (LR) modelling. The parameters of the LR models were estimated using the ordinary least squares method. The models were fit in the R environment using the STATS package (R Core Team, 2019). The predictor variables extracted from the ALS data and aerial images, three for each model, were selected by comparing all possible model candidates and then selecting the model with the smallest RMSE value.

The predictive performances associated with the LDA and LR models were assessed using leave-one-out cross-validation (LOOCV). The LDA and LR models were constructed separately for the six predictor variable groups, according to Table 3. Classifications were validated using overall accuracy (OA) and kappa-values. Corresponding regression estimates were evaluated in terms of RMSE% values, which were calculated by dividing the estimate by the observed mean, and then multiplying by 100. In the case of the LR models, the standard residual error (S_e) and coefficient of determination (R^2) were reported.

Table 4. Airborne laser scanning (ALS) and aerial image-based features, which were used as the predictor variables in the classification of fuel parameters. The classification was carried out using linear discriminant analysis (LDA). For the abbreviations, please refer to Table 2.

Remote sensing data	Fuel parameter		
	Main tree species	Site fertility	Existence of understory
Unispectral leaf-on ALS	f_hp80$_{1064}$, f_hp95$_{1064}$, l_hSkew$_{1064}$, l_iKurt$_{1064}$, l_iP95$_{1064}$	f_hP20$_{1064}$, l_hP50$_{1064}$, f_iP10$_{1064}$, f_iP20$_{1064}$, l_iP50$_{1064}$	l_hStd$_{1064}$, l_iStd$_{1064}$, l_iP30$_{1064}$, l_iP60$_{1064}$, l_iP80$_{1064}$
Unispectral leaf-on ALS and aerial images	l_iMed$_{1064}$, l_iP80$_{1064}$, aiMean$_{R}$, aiMax$_{G}$, aiMean$_{N}$		
Unispectral leaf-off ALS	f_hMean, l_hMean, l_hP90, f_iP40, f_iP90	f_hP30, l_hP60, l_hP90, l_D20, l_iP90	f_hP70, f_D5, l_D2, f_iP10, f_iP20
Unispectral leaf-off ALS and aerial images	f_hP70, l_hStd, l_iMean, aiMean$_{R}$, aiMax$_{N}$	f_iMean, f_iSkew, l_iP90, aiMin$_{N}$, aiMean$_{N}$	f_D2, l_D0.5, f_iP10, f_iP30, aiStd$_{N}$
Multispectral leaf-on ALS	l_iP20$_{1550}$, l_iP20$_{1550/1064}$, f_iStd$_{1064+532}$, l_iMean$_{1550+1064+532}$, l_iP80$_{1550+1064+532}$	l_hP60$_{1064}$, l_iP20$_{1064}$, f_D15$_{532}$, f_iP20$_{1550/1064}$, l_iP20$_{1550+1064}$	f_D20$_{1550}$, f_iP20$_{1550+532}$, int_hStd$_{1064+532}$, l_iP70$_{1064+532}$, l_iP60$_{1064/532}$
Multispectral leaf-on ALS and aerial images	l_iP60$_{1064/532}$, l_iP90$_{1550+1064+532}$, aiMean$_{R}$, aiStd$_{G}$, aiMean$_{N}$		

Results

The predictor variables in the LDA and LR models are shown in Tables 4 and 5, respectively. The role of ALS intensity features was emphasized in the classifications and they were selected by the heuristic feature selection in each case (Table 4). In addition, aerial image features were often used in the classification of main tree species. Otherwise, they were useful when combined with leaf-off unispectral ALS features in the classification of site fertility and the existence of an understory. In the classifications based on the leaf-on multispectral ALS data, multicloud and multiratio features were used more often than unispectral features. Density features were not selected as predictor variables in the models based on leaf-on unispectral ALS data. Instead, density features were used in the models that were fitted using leaf-off unispectral ALS and leaf-on multispectral ALS data for the classification of site fertility and the existence of an understory.

In the LR models, height, density and the intensity features extracted from the ALS datasets were used as predictor variables (Table 5). Height-related features were used most often but density and intensity variables were emphasized in the estimation of understory fuel parameters, i.e. the height and AGB of existing SCH. Multicloud and multiratio features were used more often than unispectral metrics in the models based on leaf-on multispectral ALS data. The different channels were all used rather evenly. In contrast, first pulse features were applied more often than last pulse features.

The role of aerial image features was very minor and, in the case of leaf-off unispectral and leaf-on multispectral ALS data, they were not used at all. The modeling of CBH in the pine stands was based on features extracted from one channel of the leaf-on ALS data. Thus, the models that used leaf-on multispectral and leaf-on unispectral ALS data are identical. On the other hand, the CBH model in the pine stands is based on canopy height and density features, whereas intensity features are included in all model alternatives in the spruce stands

The observed OA and kappa values associated with the classified fuel parameters are presented in Table 6. Site fertility and the existence of an understory layer were classified most accurately by leaf-on multispectral ALS data without aerial images the OA values being 0.62 and 0.58, respectively. For the main tree species, leaf-off unispectral ALS features combined with aerial image features resulted the greatest kappa-value (0.88). In regard to the classification of the main tree species, aerial images improved the classification accuracy in all ALS datasets. Otherwise, the usage of aerial image features improved the classification accuracy only in the models that used leaf-off unispectral ALS features as predictor variables. All in all, the main tree species was classified with high OA (0.90–0.93) and kappa-values (0.81–0.88), whereas site fertility (OA 0.86–0.89; kappa-values 0.47–0.62) and the existence of an understory (OA 0.80–0.84; kappa-values 0.47–0.58) were classified with moderate success.

The performance statistics (S_e, R^2, and cross-validated RMSE%) associated with the predictions of fuel parameters are presented in Table 7. Most of the fuel parameters were predicted with smallest RMSE% values when leaf-on multispectral ALS data features were used. As an exception, the AGB of the understory layer was predicted more accurately when leaf-off unispectral ALS features (RMSE% 57.93) were used rather than leaf-on multispectral ALS features (RMSE% 63.25). For pine stand CBH and crown biomass, the reliability was similar regardless of whether unipectral leaf-on ALS or the multi-spectral leaf-on ALS dataset was used. In general, the differences in cross-validated accuracies were usually minor (in maximum about four percentage units except in the case of the AGB of the dead trees and the AGB of the understory) between the different datasets. Aerial image features improved the accuracy in only one case: the prediction of AGB of the understory layer using unispectral leaf-on ALS features. Aerial image features were not able to improve the accuracy of the predictions, which were based on leaf-off unispectral ALS data or

Table 5. Predictor variables in the fuel parameter models. If the aerial image features did not improve the model performance, the result is the same as when airborne laser scanning (ALS) data alone was used. Fuel parameters: AGB; aboveground biomass (l = living, d = dead), SCH; surface canopy height and CBH; canopy base height. For the abbreviations, please refer to Table 2.

Remote sensing data	Response variable of fuel parameter model							
	ln(AGB_l)	AGB_d	ln (Crown biomass)	ln (Needle biomass)	Height of SCH	ln (AGB of SCH)	CBH_{pine}	ln (CBH_{spruce})
Unispectral leaf-on ALS	f_hP80_{1064}, f_hP40_{1064}, f_D5_{1064}	f_hP60_{1064}, f_hMean_{1064}, l_hP90_{1064}	f_hP95_{1064}, l_hSkew_{1064}, f_hSkew_{1064}	f_hPSkew_{1064}, l_hPSkew_{1064}, f_D5_{1064}	f_D10_{1064}, f_iMean_{1064}, l_iP80_{1064}	f_D5_{1064}, $l\_D0.5_{1064}$, l_iP95_{1064}	f_hP90_{1064}, f_hSkew_{1064}, l_D5_{1064}	f_hMean_{1064}, l_iP10_{1064}, $f\_D0.5_{1064}$
Unispectral leaf-on ALS and aerial images						f_D10_{1064}, f_hMean_{1064}, $aiMin_R$		
Unispectral leaf-off ALS	f_D5, f_hP95, f_iP70	f_D15, f_hP90, l_hP40	f_D5, f_hP70, f_hP95	f_D5, f_hSkew, l_hP30	f_iP20, l_iMean, l_iMed	f_D0.5, f_D5, f_hKurt	f_hP70, f_hSkew, l_D5	f_hP70, f_iP80, l_iP70
Unispectral leaf-off ALS and aerial images								
Multispectral leaf-on ALS	l_hSkew_{1550}, $f\_hP90_{1550+532}$, $f\_iP70_{1550+532}$	f_hMean_{1550}, $f\_hP90_{1064+532}$, $f\_hP70_{1550+1064+532}$	f_hP80_{1550}, $f\_hP95_{1064+532}$, l_hSkew_{1550}	f_D5_{1064}, $l\_hskew_{1550+532}$, $f\_hSkew_{1064+532}$	$f\_iP20_{1550+532}$, $f\_D5_{1064/532}$, $f\_D2_{1550/532}$	$f\_D2_{1550/532}$, $f\_D5_{1550/532}$, $l\_iSkew_{1064/532}$	f_hP90_{1064}, f_hSkew_{1064}, l_D5_{1064}	f_hP80_{1064}, l_hP90_{1550}, f_iMed_{1064}
Multispectral leaf-on ALS and aerial images								

Table 6. Overall accuracy (OA) and kappa values associated with the classification of fuel parameters. If aerial image features did not improve the classification accuracy, the result is the same as when airborne laser scanning (ALS) data alone was used.

Remote sensing data	Accuracy measure	Fuel parameter		
		Main tree species	Site fertility	Existence of understory
Unispectral leaf-on ALS	OA	0.90	0.86	0.82
	Kappa	0.81	0.49	0.54
Unispectral leaf-on ALS and aerial images	OA	0.92		
	Kappa	0.86		
Unispectral leaf-off ALS	OA	0.91	0.86	0.80
	Kappa	0.84	0.47	0.47
Unispectral leaf-off ALS and aerial images	OA	0.93	0.87	0.81
	Kappa	0.88	0.52	0.50
Multispectral leaf-on ALS	OA	0.92	0.89	0.84
	Kappa	0.85	0.62	0.58
Multispectral leaf-on ALS and aerial images	OA	0.93		
	Kappa	0.87		

leaf-on multispectral ALS data. The most challenging fuel parameters to be predicted were the AGB of the dead trees and the AGB of the understory layer. Total living AGB (RMSE% 17.17) and CBH by tree species (RMSE% pine 8.78 and spruce 15.18%) were the most accurately predicted parameters.

An example of wall-to-wall canopy fuel parameter prediction and classification is shown in Figure 2. The considered area also includes low stocked stands and roads. It can be seen that increasing crown biomass estimates (a) follow the corresponding trend in canopy height surface (c). Some (within stand) variation can still be observed. The existence of understory (b) does not follow the same trend. For example, there are areas with high canopy height where understory does not exist and vice versa. This is most probably due to the silvicultural history and site fertility.

Discussion

This study considers the prediction of forest canopy fuel parameters in managed middle-aged and mature boreal forests by applying remotely sensed data. Remote sensing-based predictions of canopy fuel parameters is not novel and such studies have also been conducted previously in boreal forest conditions (Bohlin et al., 2017; Morsdorf et al., 2004). However, our study concentrated on managed boreal forests with stand characteristics that are common in forested Nordic countries. Growing stock stem density in these forests is usually rather sparse due to forest management (frequent thinning) and, typically, they are not prone to fire. There has also been relatively effective fire control in Nordic countries, and forest fires, therefore, do not typically cause devastating damage. However, there have been large forest fires in Nordic countries during the latter half of the 2010s, and the risk of forest fires is expected to increase in the boreal forests of Nordic countries due to climate change (Lehtonen et al., 2014, 2016).

Another aspect in this study is the combined use of various remotely sensed datasets. The combination of low-density unispectral ALS data and aerial images has been the basic setup in Finnish operational remote sensing-based forest inventories. Aerial images are used jointly with ALS data because of the need for species-specific estimation of stand attributes (Maltamo & Packalen, 2014). In our study, the low-density ALS dataset was acquired under leaf-off conditions. Here, we separately applied multispectral ALS data and the second channel of the multispectral ALS dataset. The features extracted from the ALS datasets were also combined with aerial image features. The use of multispectral ALS data is still rare in the characterization of forest structures (see Dalponte et al., 2018).

The forest fuel-related parameters considered here include those that are often used in fuel behavior models, i.e. variables that describe CBD, CBH and canopy surface height. In addition, we consider site fertility and the biomass of both living and dead trees. As a proxy approximate for CBD, we modeled canopy fuel weight that included only needles, and needle and branch biomass. These predicted values can be converted to an estimate of CBD using canopy volume, which can be calculated from ALS data. Correspondingly, canopy surface height was described by the existence of an understory and by height and biomass of the understory.

The results pertaining to the constructed LR models were logical, and the accuracies achieved were comparable to earlier studies, for example, crown heights and biomass of living and dead trees (see Dean et al., 2009; Maltamo et al., 2014; Montagnoli et al., 2015; Næsset & Økland, 2002; Zolkos et al., 2013). Living tree biomass and crown heights were accurately predicted, whereas prediction of dead tree biomass and the understory was problematic with ALS data. Dead tree AGB cannot be considered as primary fuel parameter but biomass of understory is often needed in forest fire simulators as input parameter. Although the RMSE% values were over 50 for understory AGB it should be remembered that by absolute means the amount of understory AGB is very small (between 0.2–5.3 $Mg{\cdot}ha^{-1}$). Thus, high relative errors may not prevent the operational use of the predictions of this parameter. Crown biomass (RMSE% 21.56–22-54) was predicted with smaller errors than needle biomass (RMSE% 26.88–30.96). In regard to the applied remote sensing data, multispectral ALS provided

Table 7. Model accuracy (standard residual error (s_e) and R^2) and cross-validated root mean square error (RMSE%) values of the fuel parameter models using airborne laser scanning (ALS) and aerial image features. If the aerial image features did not improve the model performance the result is the same as when ALS data alone was used. For the abbreviations of the fuel parameters, please refer to Table 5.

Remote sensing data		Response variable of fuel parameter model							
		ln(AGB_l)	AGB_d	ln (Crown biomass)	ln (Needle biomass)	Height of SCH	ln (AGB of SCH)	CBH_{pine}	ln (CBH_{spruce})
Unispectral leaf-on ALS	s_e	0.18	2.34	0.20	0.25	4.85	0.61	0.84	0.16
	R^2	0.81	0.25	0.79	0.79	0.49	0.35	0.90	0.81
	RMSE%	18.91	265.46	21.56	29.95	24.46	70.60	8.78	16.69
Unispectral leaf-on ALS and aerial images	s_e						0.580		
	R^2						0.40		
	RMSE%						67.77		
Unispectral leaf-off ALS	s_e	0.18	2.36	0.20	0.24	5.04	0.56	0.93	0.18
	R^2	0.81	0.23	0.80	0.79	0.45	0.44	0.88	0.77
	RMSE%	18.66	249.22	22.54	30.96	24.65	57.93	9.91	16.88
Unispectral leaf-off ALS and aerial images	s_e								
	R^2								
	RMSE%								
Multispectral leaf-on ALS	s_e	0.17	2.22	0.20	0.23	4.21	0.57	0.84	0.16
	R^2	0.83	0.32	0.80	0.82	0.61	0.42	0.90	0.83
	RMSE%	17.17	239.77	21.56	26.88	20.62	63.25	8.78	15.18
Multispectral leaf-on ALS and aerial images	s_e								
	R^2								
	RMSE								

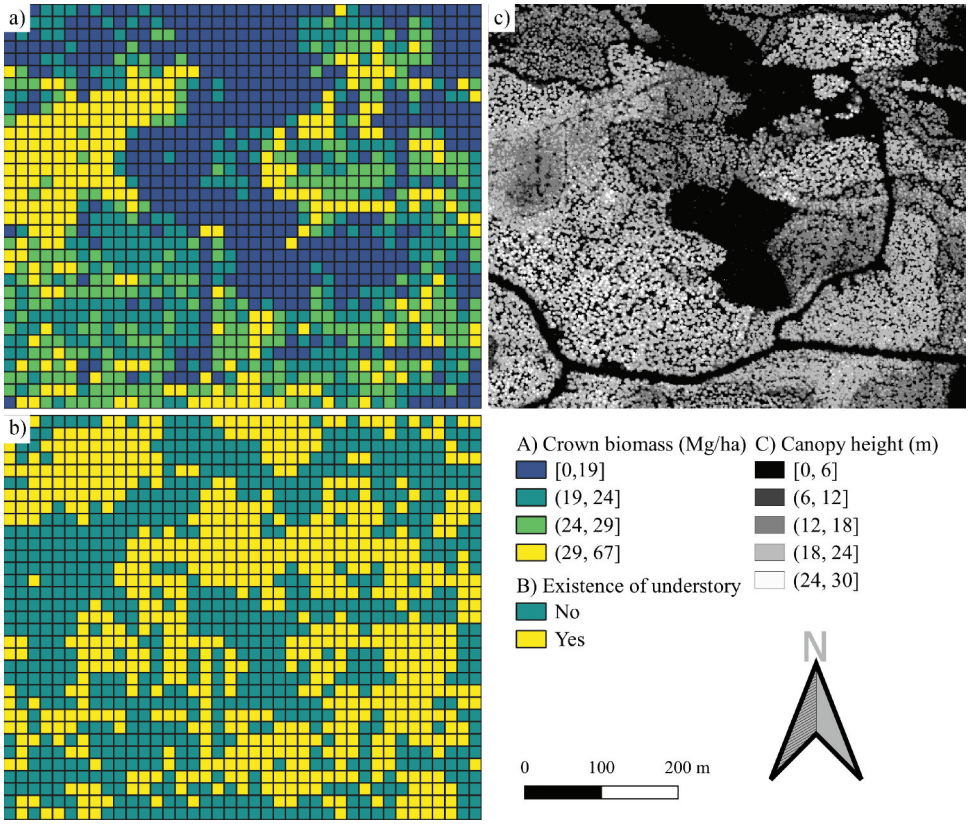

Figure 2. An example of the wall-to-wall canopy fuel parameter prediction and classification using a cell size of 16 ×16 m and multispectral ALS data. The layers are (a) the crown biomass (Mg·ha^{-1}) and (b) the existence of understory (yes-no). The canopy height above ground level using a pixel size of 1 m is also presented from the same area (c).

slightly more accurate (less than about four percentage units in RMSE%) results than the other alternatives in most cases. This is partly contrary to previous studies where species-specific attributes were not predicted as accurately by multispectral data as by the combination of ALS and aerial images (e.g. Kukkonen et al., 2019a).

In our study, the role of aerial image features was minor. Still, the differences between the various ALS options were not large. On the other hand, Dalponte et al. (2018) predicted aboveground biomass per hectare and the number of trees per hectare by means of multispectral ALS data (Optech Titan). They reported that multispectral ALS data outperforms unispectral ALS data in terms of predictive performance, which is in line with our results.

The classification of dominant tree species was successful. The obtained kappa-values were always greater than 0.8. Also, this result is in agreement with earlier studies (Kukkonen et al., 2019b; Räty et al., 2019), which showed that the inclusion of aerial image features improves classification (0.04–0.08 difference in kappa-value) and prediction accuracy (0.4–9.5 percentage units) for different forest variables. It is also notable that multispectral data was not the most accurate alternative in this case, as the use of unispectral leaf-off ALS data in combination with aerial images achieved higher classification accuracy. In the context of forest fuel parameters, dominant tree species information is not of primary interest but is needed to separate pine and spruce dominated stands in crown base height predictions. The other classifications – site fertility and the existence of an understory – were classified with kappa-values between 0.47–0.62 and, in these cases, multispectral ALS data again achieved a higher classification accuracy than the unispectral ALS datasets. It should be noted that we only applied two classes for site fertility in this study: fire-prone dry forests and less fire-prone, more fertile forests, which clearly improved the classification problem, in comparison to earlier studies (Vehmas et al., 2011).

Our models contained a large number of candidate predictor variables. One aspect here is the type of multispectral features that were applied. It would seem that the ratio features between the different channels of the multispectral ALS data were frequently used as predictor variables in models that predicted understory parameters. Ratio features were also common in the models that we used to classify the main tree species and site fertility. Features that combined different channels were more frequently applied in almost all models and classifications. The role of intensity features was more important in the classification of categorical parameters than in the prediction of continuous forest parameters. For continuous forest parameters, the intensity features were only applied in

the prediction of the understory and in the crown base height models. The intensity features were also more frequently used in the classification of categorical parameters than in the prediction of continuous forest parameters with datasets other than multispectral ALS.

Conclusions

We studied the prediction of fuel-related forest parameters using different ALS datasets and aerial imagery. The findings showed that multispectral ALS data outperformed the unispectral ALS data in the prediction of forest fuel parameters. This indicates the usefulness of multispectral ALS data for the prediction of forest structure parameters.

Of the considered fuel-related variables, the most important forest fuel parameters, i.e. CBD (canopy weight), CBH and canopy surface height attributes, were successfully predicted, with the exception of the understory biomass. The classification of forest fertility classes was also successful.

To conclude, the prediction of the most critical fuel parameters was generally successful and the obtained accuracies are adequate for operational use. Our findings can also be directly utilized in the applications of forest fuel models, particularly in Finland, but also in other Nordic countries.

Disclosure statement

No potential conflict of interest was reported by the authors.

Funding

This work was supported by the Strategic Research Council of the Academy of Finland for the FORBIO project (decision number 314224), led by Prof. Heli Peltola at the School of Forest Sciences, University of Eastern Finland.

References

Andersen, H. E., McGaughey, R. J., & Reutebuch, S. E. (2005). Estimating forest canopy fuel parameters using LIDAR data. *Remote Sensing of Environment*, *94*(4), 441–449. https://doi.org/10.1016/j.rse.2004.10.013

Arroyo, L. A., Pascual, C., & Manzanera, J. A. (2008). Fire models and methods to map fuel types: The role of remote sensing. *Forest Ecology and Management*, *256*(6), 1239–1252. https://doi.org/10.1016/j.foreco.2008.06.048

Axelsson, A., Lindberg, E., & Olsson, H. (2018). Exploring multispectral ALS data for tree species classification. *Remote Sensing*, *10*(2), 183. https://doi.org/10.3390/rs10020183

Axelsson, P. (2000). DEM generation from laser scanner data using adaptive TIN models. *International Archives of the Photogrammetry, Remote Sensing and Spatial Information Sciences*, *33*(B4/1), 110–117.

Bohlin, I., Olsson, H., Bohlin, J., & Granström, A. (2017). Quantifying post-fire fallen trees using multi-temporal lidar. *International Journal of Applied Earth Observation and Geoinformation*, *63*, 186–195. https://doi.org/10.1016/j.jag.2017.08.004

Budei, B. C., St-Onge, B., Hopkinson, C., & Audet, F. (2018). Identifying the genus or species of individual trees using a three-wavelength airborne lidar system. *Remote Sensing of Environment*, *204*(1), 632–647. https://doi.org/10.1016/j.rse.2017.09.037

Cajander, A. K. (1926). The theory of forests types. *Acta Forestalia Fennica*, *29*(3), 1–108. https://doi.org/10.14214/aff.7193

Chirici, G., Scotti, R., Montaghi, A., Barbati, A., Cartisano, R., Lopez, G., Marchetti, M., McRoberts, R. E., Olsson, H., & Corona, P. (2013). Stochastic gradient boosting classification trees for forest fuel types mapping through airborne laser scanning and IRS LISS-III imagery. *International Journal of Applied Earth Observation and Geoinformation*, *25*, 87–97. https://doi.org/10.1016/j.jag.2013.04.006

Dalponte, M., Ene, L. T., Gobakken, T., Næsset, E., & Gianelle, D. (2018). Predicting selected forest stand characteristics with multispectral ALS data. *Remote Sensing*, *10*(4), 586. https://doi.org/10.3390/rs10040586

Dean, T. J., Cao, Q. V., Roberts, S. D., & Evans, D. L. (2009). Measuring heights to crown base and crown median with LiDAR in a mature, even-aged loblolly pine stand. *Forest Ecology and Management*, *257*(1), 126–133. https://doi.org/10.1016/j.foreco.2008.08.024

Erdody, T. L., & Moskal, L. M. (2010). Fusion of LiDAR and imagery for estimating forest canopy fuels. *Remote Sensing of Environment*, *114*(4), 725–737. https://doi.org/10.1016/j.rse.2009.11.002

Esseen, P. A., Ehnström, B., Ericson, L., & Sjöberg, K. (1997). Boreal forests. *Ecological Bulletins*, *46*, 16–47.

Estornell, J., Ruiz, L. A., & Velazquez-Marti, B. (2011). Study of shrub cover and height using LIDAR data in a mediterranean area. *Forest Science*, *57*, 171–179.

Finney, M. A. (1998). FARSITE: Fire area simulator - Model development and evaluation. USDA Forest Service Rocky Mountain Forest and Range Experiment Station Research Paper.

Forest Europe. (2015). *State of Europe's forests 2015 ministerial conference on the protection of forests in Europe*

Gajardo, J., García, M., & Riaño, D. (2014). Applications of airborne laser scanning in forest fuel assessment and fire prevention. In M. Maltamo, E. Naesset, & J. Vauhkonen (Eds.), *Forestry applications of airborne laser scanning – concepts and case studies. Managing forest ecosystems* (Vol. 27, pp. 439–462). Springer. https://geo3d.hr/sites/default/files/2018-06/Titan-Specsheet-150515-WEB.pdf

Hauglin, M., Gobakken, T., Lien, V., Bollandsås, O. M., & Næsset, E. (2012). Estimating potential logging residues in a boreal forest by airborne laser scanning. *Biomass & Bioenergy*, *36*, 356–365. https://doi.org/10.1016/j.biombioe.2011.11.004

Hill, R. A., & Broughton, R. K. (2009). Mapping the understorey of deciduous woodland from leaf-on and leaf-off airborne LiDAR data: A case study in lowland Britain. *ISPRS Journal of Photogrammetry and Remote Sensing*, *64*(2), 223–233. https://doi.org/10.1016/j.isprsjprs.2008.12.004

Holsinger, L., Parks, S. A., & Miller, C. (2016). Weather, fuels, and topography impede wildland fire spread in western US landscapes. *Forest Ecology and Management*, *380*, 56–69. https://doi.org/10.1016/j.foreco.2016.08.035

Jones, H. G., & Vaughan, R. A. (2012). Remote sensing of vegetation: Principles, techniques, and applications. *The Quarterly Review of Biology*, *87*(2), 165–166.

Kirkpatrick, S., Gelatt, C. D., & Vecchi, M. P. (1983). Optimization by simulated annealing. *Science*, *220*(4598), 671–680. https://doi.org/10.1126/science.220.4598.671

Korpela, I., Orka, H. O., Hyyppä, J., Heikkinen, V., & Tokola, T. (2010). Range and AGC normalization in airborne discrete-return LiDAR intensity data for forest canopies. *ISPRS Journal of Photogrammetry and Remote Sensing*, *65*(4), 369–379. https://doi.org/10.1016/j.isprsjprs.2010.04.003

Kotamaa, E., Tokola, T., Maltamo, M., Packalén, P., Kurttila, M., & Mäkinen, A. (2010). Integration of remote sensing-based bioenergy inventory data and optimal bucking for stand-level decision making. *European Journal of Forest Research*, *129*(5), 875–886. https://doi.org/10.1007/s10342-010-0357-4

Koutsias, N., & Karteris, M. (2003). Classification analyses of vegetation for delineating forest fire fuel complexes in a Mediterranean test site using satellite remote sensing and GIS. *International Journal of Remote Sensing*, *24*(15), 3093–3104. https://doi.org/10.1080/0143116021000021152

Kukkonen, M., Maltamo, M., Korhonen, L., & Packalen, P. (2019a). Comparison of multispectral airborne laser scanning and stereo matching of aerial images as a single sensor solution to forest inventories by tree species. *Remote Sensing of Environment*, *231*, 111208. https://doi.org/10.1016/j.rse.2019.05.027

Kukkonen, M., Maltamo, M., Korhonen, L., & Packalen, P. (2019b). Multispectral airborne LiDAR data in the prediction of boreal tree species composition. *IEEE Transactions on Geoscience and Remote Sensing*, *57*(6), 3462–3471. https://doi.org/10.1109/TGRS.2018.2885057

Lehtonen, I., Ruosteenoja, K., Venäläinen, A., & Gregow, H. (2014). The projected 21st century forest fire risk in Finland under different greenhouse gas scenarios. *Boreal Environment Research*, *19*(2), 127–139. http://hdl.handle.net/10138/228540

Lehtonen, I., Venäläinen, A., Kämäräinen, M., Peltola, H., & Gregow, H. (2016). Risk for large-scale fires in boreal forests of Finland under changing climate. *Natural Hazards and Earth Systems Sciences*, *16*(1), 239–253. https://doi.org/10.5194/nhess-16-239-2016

Lim, K. S., & Treitz, P. M. (2004). Estimation of above ground forest biomass from airborne discrete return laser scanner data using canopy-based quantile estimators. *Scandinavian Journal of Forest Research*, *19*(6), 558–570. https://doi.org/10.1080/02827580410019490

Maltamo, M., Bollandsås, O. M., Vauhkonen, J., Breidenbach, J., Gobakken, T., & Næsset, E. (2010). Comparing different methods for prediction of mean crown height in Norway spruce stands using airborne laser scanner data. *Forestry*, *83*(3), 257–268. https://doi.org/10.1093/forestry/cpq008

Maltamo, M., Kallio, E., Bollandsås, O. M., Næsset, E., Gobakken, T., & Pesonen, A. (2014). Assessing dead wood by airborne laser scanning. In M. Maltamo, E. Naesset, & J. Vauhkonen (Eds.), *Forestry applications of airborne laser scanning –concepts and case studies. Managing forest ecosystems* (Vol. 27, pp. 375–395). Springer.

Maltamo, M., Karjalainen, T., Repola, J., & Vauhkonen, J. (2018). Incorporating tree- and stand-level information on crown base height into multivariate forest management inventories based on airborne laser scanning. *Silva Fennica*, *52*(3), article id 10006. https://doi.org/10.14214/sf.10006

Maltamo, M., & Packalen, P. (2014). Species specific management inventory in Finland. In M. Maltamo, E. Naesset, & J. Vauhkonen (Eds.), *Forestry applications of airborne laser scanning –concepts and case studies. Managing forest ecosystems* (Vol. 27, pp. 241–252). Springer.

Maltamo, M., Packalén, P., Yu, X., Eerikäinen, K., Hyyppä, J., & Pitkänen, J. (2005). Identifying and quantifying structural characteristics of heterogeneous boreal forests using laser scanner data. *Forest Ecology and Management*, *216*(1–3), 41–50. https://doi.org/10.1016/j.foreco.2005.05.034

Merrill, D. F., & Alexander, M. E. (1987). *Glossary of forest fire management terms*. National Research Council of Canada, Committee for Forest Fire Management.

Miura, N., & Jones, S. D. (2010). Characterizing forest ecological structure using pulse types and heights of airborne laser scanning. *Remote Sensing of Environment*, *114*(5), 1069–1076. https://doi.org/10.1016/j.rse.2009.12.017

Montagnoli, A., Fusco, S., Terzaghi, M., Kirsrchbaum, A., Pflugmacher, D., Cohen, W. B., Scippa, G. S., & Chiatanrte, D. (2015). Estimating forest aboveground biomass by low density lidar data in mixed broad-leaved forests in Italian Pre-Alps. *Forest Ecosystems*, *2*(1), 10. https://doi.org/10.1186/s40663-015-0035-6

Moritz, M. A., Hessburg, P. F., & Povak, N. A. (2011). Native fire regimes and landscape resilience. In D. McKenzie, C. Miller, & D.A. Falk (Eds.), *The landscape ecology ofFire* (pp. 51–86). Springer.

Morsdorf, F., Meier, E., Kötz, B., Itten, K. I., Dobbertin, M., & Allgöwer, B. (2004). LIDAR-based geometric reconstruction of boreal type forest stands at single tree level for forest and wildland fire management. *Remote Sensing of Environment*, *92*(3), 353–362. https://doi.org/10.1016/j.rse.2004.05.013

Mutlu, M., Popescu, S. C., Stripling, C., & Spencer, T. (2008). Mapping surface fuel models using lidar and multispectral data fusion for fire behavior. *Remote Sensing of Environment*, *112*(1), 274–285. https://doi.org/10.1016/j.rse.2007.05.005

Næsset, E., & Økland, T. (2002). Estimating tree height and tree crown properties using airborne scanning laser in a boreal nature reserve. *Remote Sensing of Environment*, *79*(1), 105–115. https://doi.org/http://dx.doi.10.1016/S0034-4257(01)00243-7

Peterson, B., Dubayah, R., Hyde, P., Hofton, M., Blair, J. B., & Fites-Kaufman, J. (2007). Use of LIDAR for forest inventory and forest management application. In R. McRoberts, G. Reams, P. Van Deusen, & W. H. McWilliams (Eds.). *Proceedings of the seventh annual forest inventory and analysis symposium*, October 3-6, 2005, Portland, ME. *General Technical Report*, WO-77, (pp. 193–202). Washington DC: U.S. Department of Agriculture, Forest Service.

R Core Team. (2019). *R: A language and environment for statistical computing*. R Foundation for Statistical Computing. https://www.R-project.org/.

Räty, J., Packalen, P., & Maltamo, M. (2019). Nearest neighbor imputation of logwood volumes using Bi-temporal ALS, multispectral ALS and aerial images. *Scandinavian Journal of Forest Research*, *34*(6), 469–483. https://doi.org/10.1080/02827581.2019.1589567

Repola, J. (2008). Biomass equations for birch in Finland. *Silva Fennica*, *42*(4), 605–624. https://doi.org/10.14214/sf.236

Repola, J. (2009). Biomass equations for Scots pine and Norway spruce in Finland. *Silva Fennica*, *43*(4), 625–647. https://doi.org/10.14214/sf.184

Riaño, D., Chuvieco, E., Ustin, S. L., Salas, J., Rodriguez-Perez, J. R., Ribeiro, L. M., Viegas, D. X., Moreno, J. M., & Fernández, H. (2007). Estimation of shrub height for fuel-type mapping combining airborne LiDAR and simultaneous color infrared ortho imaging. *International Jornal of Wildland Fire*, *16*(3), 341–348. https://doi.org/10.1071/WF06003

Riaño, D., Meier, E., Allgower, B., Chuvieco, E., & Ustin, S. L. (2003). Modeling airborne laser scanning data for the spatial generation of critical forest parameters in fire behavior modeling. *Remote Sensing of Environment*, *86*(2), 177–186. https://doi.org/10.1016/S0034-4257(03)00098-1

Ruosteenoja, K., Markkanen, T., Venäläinen, A., Räisänen, P., & Peltola, H. (2018). Seasonal soil moisture and drought occurrence in Europe in CMIP5 projections for the 21st century. *Climate Dynamics*, *50*(3–4), 1177–1192. https://doi.org/10.1007/s00382-017-3671-4

Salminen, H., Lehtonen, M., & Hynynen, J. (2005). Reusing legacy FORTRAN in the MOTTI growth and yield simulator. *Computational Electronics in Agriculture*, *49*(1), 103–113. https://doi.org/10.1016/j.compag.2005.02.005

Seielstad, C. A., & Queen, L. P. (2003). Using airborne laser altimetry to determine fuel models for estimating fire behavior. *Journal of Forestry*, *101*(4), 10–15. https://doi.org/10.1093/jof/101.4.10

Sumnall, M., Hill, R. A., & Hinsley, S. A. (2016). Comparison of small-footprint discrete return and full waveform airborne lidar data for estimating multiple forest variables. *Remote Sensing of Environment*, *173*, 214–223. https://doi.org/10.1016/j.rse.2015.07.027

Valbuena, R., Eerikäinen, K., Packalen, P., & Maltamo, M. (2016). Gini coefficient predictions from airborne lidar remote sensing display the effect of management intensity on forest structure. *Ecological Indicators*, *60*, 574–585. https://doi.org/10.1016/j.ecolind.2015.08.001

Vauhkonen, J. (2010). Estimating crown base height for Scots pine by means of the 3-D geometry of airborne laser scanning data. *International Journal of Remote Sensing*, *31*(5), 1213–1226. https://doi.org/10.1080/01431160903380615

Vehmas, M., Eerikäinen, K., Peuhkurinen, J., Packalén, P., & Maltamo, M. (2011). Airborne laser scanning for the site type identification of mature boreal forest stands. *Remote Sensing*, *3*(1), 100–116. https://doi.org/10.3390/rs3010100

Venables, W. N., & Ripley, B. D. (2002). *Modern applied statistics with S* (4th ed.). Springer.

Wall, T., Fröblom, J., Kilpeläinen, H., Lindblad, J., Heikkilä, A., Song, T., Stöd, R., & Verkasalo, E. (2004). *Harvennusmännyn hankinnan ja sahauksen kehittäminen*. [Developing the procurement and sawing of thinned scots pine trees]. *Wood Wisdom – Tutkimusohjelman hankekonsortion julkinen loppuraportti*. Laaja versio. [In Finnish]. Finnish Forest Research Institute, Joensuu Research Unit.

Yu, X., Hyyppä, J., Litkey, P., Kaartinen, H., Vastaranta, M., & Holopainen, M. (2017). Single-sensor solution to tree species classification using multispectral airborne laser scanning. *Remote Sensing*, *9*(2), 108. https://doi.org/10.3390/rs9020108

Zolkos, S. G., Goetz, S. J., & Dubayah, R. (2013). A meta-analysis of terrestrial aboveground biomass estimation using lidar remote sensing. *Remote Sensing of Environment*, *128*, 289–298. https://doi.org/10.1016/j.rse.2012.10.017